Available online at www.sciencedirect.com

ScienceDirect

journal homepage: www.keaipublishing.com/jtte

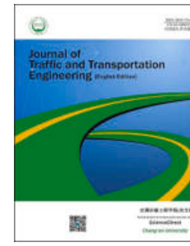

Original Research Paper

Laboratory surface texture analysis of road pavements using a mobile phone camera based close-range photogrammetry technique

Filippo Balzano[a,*], *Piergiorgio Tataranni*[a], *David Woodward*[b], *Cesare Sangiorgi*[a]

[a] *Department of Civil, Chemical, Environmental and Materials Engineering, University of Bologna, Bologna 40136, Italy*
[b] *Belfast School of Architecture and the Built Environment, Ulster University, Belfast, BT15 1AP, Northern Ireland, UK*

HIGHLIGHTS

- Surface texture is a very strategic parameter to assess road pavements performance.
- Close-range photogrammetry can provide an in-depth surface texture characterization.
- 3D-modelling allows describing pavement status for maintenance and design purposes.

ARTICLE INFO

Article history:
Received 24 May 2024
Received in revised form
26 November 2024
Accepted 10 December 2024
Available online 4 June 2025

Keywords:
Surface texture
Road pavements
Close-range photogrammetry
Pavement maintenance
Abbott-firestone curve

ABSTRACT

The wearing course conditions strongly affect road pavements quality in terms of traffic safety and overall functionality. Surface texture can be considered a very strategic aspect to assess road pavement status, in order to predict its degradation and to define an effective maintenance program. Nowadays, common texture assessment approaches are mainly empirical and based on in-situ and/or laboratory direct measurements, thus the quantity and quality of the obtainable information are limited. On the other hand, advanced contactless techniques require expensive and often complicated equipment that can be hardly used in common applications. In this regard, a low budget close-range photogrammetry technique for road pavements 3D surface texture analysis is here proposed. 14 areal texture parameters including depth, volume, distribution and feature indicators have been determined by analysing the 3D models. The outcomes have been compared with those found with the traditional volumetric patch and pendulum tests, and a complete pairwise correlation matrix has been obtained. Volume patch test exhibits a high relationship with different volume and height surface texture parameters, while low-correlations have been found comparing pendulum test with the intrinsic and statistical indicators. The results and their relationships have been commented in-depth along with proposed further research activities.

* Corresponding author.
E-mail addresses: filippo.balzano2@unibo.it (F. Balzano), piergiorg.tataranni2@unibo.it (P. Tataranni), wdh.woodward@ulster.ac.uk (D. Woodward), cesare.sangiorgi4@unibo.it (C. Sangiorgi).

Peer review under responsibility of Chang' an University
https://doi.org/10.1016/j.jtte.2024.12.004

1. Introduction

1.1. *Surface texture*

Quantity and quality of road infrastructures influence the social-economic development of an urban area (Queiroz et al., 1994). On one hand, pavements can be considered the main element of road assets and must provide a solid structure to withstand the loads inducted by traffic during their service life (Afonso et al., 2019). On the other hand, the wearing course conditions strongly affect the non-structural aspects related to traffic safety and functionality, influencing pavement-tire interaction in terms of adhesion and hysteresis generated (Luo et al., 2023). In this regard, it is possible to define texture as the pavement surface deviation from a true planar reference surface (National Academies of Science Engineering and Medicine, 2009). Pavement texture is a result of the mixing and laying of the concrete made of binder (bitumen, bituminous emulsion, resin, cement, etc), mineral and/or active fillers and aggregates. Mix design also plays a major role in surface texture appearance (Woodward and Friel, 2017). Moreover, texture properties strongly evolve with time and ignoring the effects of these factors can cause the development of cracks and other forms of distresses that, if not promptly addressed, can escalate and compromise road stability and traffic safety. Texture may be considered a very strategic parameter to analyse road pavements and to assess intrinsic properties like friction (Boscaino et al., 2002), noise-generation (Miljković et al., 2014) and surface drainage (Li et al., 2024; Noyce et al., 2005). Based on the profile's wavelength λ, it is usually possible to identify different metrical ranges and to classify the pavement surface texture. In particular, with the term "micro-texture" it is possible to refer to those profiles in which $\lambda < 0.5$ mm and with "macro-texture" to those where $0.5 \text{ mm} < \lambda < 50$ mm (Cafiso and Taormina, 2007). Micro-texture is highly related to skid resistance (Vaiana et al., 2019) as well to other phenomena of molecular adhesion, and it also depends on the physical and mineral characteristics of the aggregates (Yu et al., 2020). On the contrary, macro-texture is the result of the inter-granular roughness, connected with the particle size distribution and, in general, with the number of peaks/valleys appearing on the outer surface. Besides increasing the general grip offered on the top surface of pavement, as a result of the hysteresis energy dissipated on aggregates by tires (Fernando et al., 2023), macro-texture significantly influences noise generation (Callai and Sangiorgi, 2021; Canestrari et al., 2024) and water drainage (Afonso et al., 2019). It is worth to observe how all above listed phenomena can be ascribed as functional performances associated to users' safety and driving comfort, so it is clearly understandable how a higher knowledge of texture characteristics could lead to a better description of pavement surface status, aiming to anticipate degradation phenomena and to define an effective management and maintenance program.

1.2. *Methods for surface texture assessment*

Nowadays, the common approaches for pavement surface texture assessment are mainly empirical and based on in-situ and/or laboratory measurements (Cafiso and Taormina, 2007). Volumetric sand patch method is the most used one to determine the macro-texture on road pavements (Yu et al., 2023; Yun et al., 2025), mainly because of the simple test operations and the intuitiveness of results. Alternatively, permeability-related methods are common and involve the use of outflow meters (Cooley, 1999). Generally, micro-texture is not directly measured and it is replaced by friction evaluations (Cesbron et al., 2008). Devices such as the British pendulum tester, the dynamic friction tester and the locked-wheel skid trailer are today mostly used for micro-texture investigations (Chu et al., 2019; Gu et al., 2022; Leng et al., 2023). These indirect determination approaches have seen a large diffusion since they involve low budget equipment and do not require specialized personnel to be performed. However, the other side of the coin is a large discreteness of test results and, often, an unsatisfactory representativeness of the overall pavement quality (Hao et al., 2016). In addition, empirical tests are based on extrinsic criteria, aiming to describe surface texture by measuring quantities directly related to it. Since surface texture is a complex shape where undulations with different wavelengths coexists simultaneously, the results of direct tests may be often not sensitive enough to distinguish the contribution of micro- and macro-texture to the overall profile, giving information that could be ambiguous if not properly addressed. In the recent years, the technological and scientific advancements led to the development of innovative devices for the contactless evaluation of surface texture. Non-contact analysis methods are currently applied in various engineering fields, as integration or evolution of the available measurement systems (Pranjić and Deluka-Tibljaš, 2022). In road engineering, the digitalization of results opens news perspectives in the description of pavement surface properties for design and maintenance purposes (Ban et al., 2022). Laser-based profilometers have soon become common in advanced research laboratories for their reliability on texture description (Praticò et al., 2003). These devices project a monochromatic filtered light on the pavement surface and receive its reflection back with a different angle (Boscaino et al., 2002a), obtaining by triangulation a *xz* position-depth matrix that correspond to the 2D profile of the analysed section (Bitelli et al., 2012). Due the extremely high in-build quality, it is possible to increase the acquisition rate up to obtain a step distance of 1–5 μm (Vaiana et al., 2019), which is reflected in highly-accurate data. The mean texture depth (MTD), mean profile depth (MPD) and estimate texture depth (ETD) are the most common parameters adopted for laser devices 2D surface texture analysis (Praticò and Vaiana, 2015). Since two-dimensional profiles may be sensitive to the position and the orientation of section, frequently they are not representative of the whole surface. In this regard, 3D laser scanners have been developed to represent a natural evolution of profilometers (Mathavan et al., 2015) for three-dimensional characterization of surfaces. Areal roughness parameters allow a deeper knowledge of texture morphology and they usually include height (root mean square height, arithmetic mean height, skewness, etc), volume (void volume, material volume, etc) and other feature texture (density or peaks/valleys, curvature, etc) parameters (Kogbara et al., 2018). 3D laser technology provides high-precision and high-speed measurements, but it requires specialized technicians to be applied, due the complexity of the equipment. Moreover, laser devices are expensive (10–100 k€ (Praticò and Vaiana, 2015)) and this brings to their limited usability in common applications (Kogbara et al., 2018). In the light of this, image-based solutions are becoming increasingly popular in pavement engineering (Mathavan et al., 2015).

1.3. *Image-based methods for texture analysis*

The general principle of all image-based methods is the acquisition of a high-precision model that accurately reflects the research object (Medeiros et al., 2021), in order to extract a dense list of morphological data to complement surface texture analysis. These can be generally divided in model-based and view-based methods (Gao and Dai, 2014): the former allow to capture features from the object-level perspective; the latter consider each three-dimensional subject as a collection of bi-dimensional projections from several viewpoints (Ansary et al., 2007). View-based methods have been highly investigated in a wide range of metrological applications (Biao et al., 2015; Li et al., 2008) and their effectiveness and flexibility have been proved over model-based ones (Hoang, 2019; Liu et al., 2021). In addition, view-based exceed model-based methods in terms of precision, reliability and versatility (Ioannidou et al., 2017). These methods apply different deep-learning algorithms to determine the coordinates of a point in the space based on its relative position within the pictures, taken from different angles (Leng et al., 2016), generating a 3D point cloud expressed through a multi-dimensional matrix. Architectures behind this process may be different, but generally convolutional neutral networks (CNN) overclass other algorithms, since they allow to handle information contained in each view simultaneously, avoiding data loss during their elaboration (Leng et al., 2016). As for pavement engineering, the concept of view-based analysis was already introduced in 1970s, when different researchers used an analog camera and a stereograph to analyse height, width and angularity of surface texture based on predefined tables (Medeiros et al., 2021). The evolution of this technique, with the advent of digital cameras, led to the so-called close-range photogrammetry (CRP). CRP exploits a software-based technology to perform a series of pairwise image elaborations, which are commonly performed using structure from motion (SfM) pipeline algorithms. Two images are rotated, translated and overlapped until the best matching configuration between keypoints is found. The shifted distances are defined as disparities and are used by software to calculate relative distances and depths by triangulation, considering the distance from camera in each photograph. Images are organized into a logical tree with agglomerative clusters, breaking the complex matching problem in a series of smaller instances, which are then separately solved and combined. CRP has been found to be a valid alternative to laser devices (Dong et al., 2022), since it may involve an ordinary camera to be performed (Kogbara et al., 2016) and it requires limited operator skills to obtain detailed and reliable results (Chen et al., 2019). However, the lighting conditions, the perspective distortion and the exposure of photographs may generate flaws in the method introducing thermal-noise, micro-blur or shadow/spikes of light effects if not accurately controlled by the operator, affecting the average quality of the generated model (Ramírez-Hernández et al., 2020). It has been recognized that cameras and lenses of high metric quality provide best results in terms of accuracy (Luhmann et al., 2016). For these reasons, a professional full-frame DSLR/Mirrorless camera, a prime normal lens and a controlled external lighting system should be adopted to avoid systematic errors in the application of the method, but the total cost of this equipment might sometimes reach the one of an entry-level laser device, limiting the diffusion of this technique to specialized laboratories. However, self-calibration algorithms are also well-proven to be reliable to recover the quality gap when a not professional equipment is involved, by acting on lightning setup and increasing the image networks (Luhmann et al., 2016).

In the light of the above, a simplified low-budged CRP approach is here proposed. The main aim of this study is to present a complete workflow for the implementation of an ordinary camera-based CRP technique as a tool for laboratory and in-situ three-dimensional description of surface texture in pavement applications. A complete data acquisition procedure is defined and calibrated to close the quality gap with professional equipment. The methodology was then applied on a wide range of different real road pavement surfaces, leading to an in-depth areal topographic analysis of their texture. Thus, the outcomes have been compared for validation with two selected empirical methodologies based on standard approaches such as the volumetric patch test (CEN, 2010) and the pendulum test (CEN, 2011), commonly used for macro-texture and micro-texture measurement respectively. A thorough pairwise correlation comparison between empirical and digital indicators was performed and discussed.

2. Materials and methods

2.1. *Materials*

In order to extend the field of applicability of the proposed methodology, a number of different road pavement surface layers were investigated. All the materials refer to real in-field applications and present different surface textures, showing a high variability in terms of aggregate type, gradation curve, binder type and production temperature. A total of 45 specimens was considered for this research and grouped according to their most notable property as shown in Table 1.

Table 1 – Sample's classification in terms of texture and colour of the binder.

Surface	Classification	*n* of specimens
Texture	Coarse	16
	Medium	28
	Fine	1
Colour	Black	38
	Coloured	2
	Transparent	5

Coarse to fine textured specimens were selected to investigate the possible effect of shadowing in the method, due to a different reorganization of peaks/valleys on the tested surfaces. Specimens were grouped following the result of volumetric patch test and later discussed.

In addition, black and lighter mixtures were included in the study to consider the rule of light reflection and thermal noise on the camera sensor in high ISO conditions. Black binder group refers to mixtures presenting bitumen, polymer modified bitumen or bituminous emulsion in the mix design. Transparent and coloured binder groups include those specimens realized with non-bituminous binders, such as polyolefin-based synthetic binders and pigmented resins.

All the specimens were laboratory compacted by means of a gyratory compactor, in accordance with EN 12697-31, and consist in regular cylinders with a diameter of 150 ± 0.1 mm and different thicknesses varying between 45 and 110 mm. The upper surface of all specimens was perpendicular to the cylinder's longitudinal axis and its top surface round edge was undamaged and clean.

2.2. Methods

This section aims to describe the methodological approach followed in this study. The experimental specimens were manufactured as described above. Their top surfaces were photographed with a standardized procedure and a set of images was saved for each specimen. Each set of images was elaborated in order to create a high-resolution 3D model of the specimen's surface. The models were analysed digitally and a list of texture parameters was obtained. Two common empirical tests were also performed on the same surfaces: the "volumetric patch test" and the "pendulum test" were selected for the macro- and micro-texture evaluation, respectively, due their common use for in-field and laboratory characterization of road pavements. In the end, results of image-based and conventional approaches were compared and valid correlations were found. The flow chart in Fig. 1 shows the main phases of the methodology followed in this study:

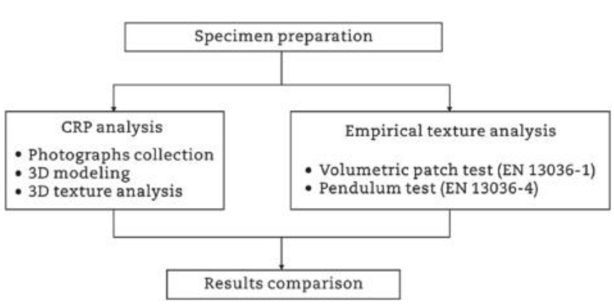

Fig. 1 – Flow chart of the experimental methodology.

2.3. Close-range photogrammetry analysis

Generally, diffused CRP techniques may require professional equipment and an intermediate level of photographic knowledge to be correctly performed (Ban et al., 2022; Kogbara et al., 2018; Pranjić and Deluka-Tibljaš, 2022), starting from the original purpose of this study. In this regard, the entire image database was collected using a common 12-megapixel mobile smartphone camera (iPhone 14). Due the limited flexibility of the in-built software of the camera in terms of EXIF parameter's manual control, a low-cost external lighting system was set up to keep the exposure conditions constant during the entire photography phase. This consisted in a hand-crafted lightbox, shown in Fig. 2.

- Three external lamps on the sides of the box made with white paper-diffusers.
- A steady and levelled housing on the top roof of the lightbox, to lock the position and the angle of the smartphone in each photo.
- A white background at the bottom of the box, to ease the identification of the surface.

The three-lamps system, in combination with the neutral soft diffusers, was needed to replicate the normal diffuse lightning under the sun, aiming to transfer this technique for in-situ applications, avoiding any direct artificial light source exposure that may cause sharp shadows and/or mirror reflections on the surface. The choice of the different bulbs was driven by the targeted natural light temperature (5500 ± 500 K) inside the box, in order to preserve the same white balance and original colours for each specimen, without resorting to external image post-production software. The smartphone

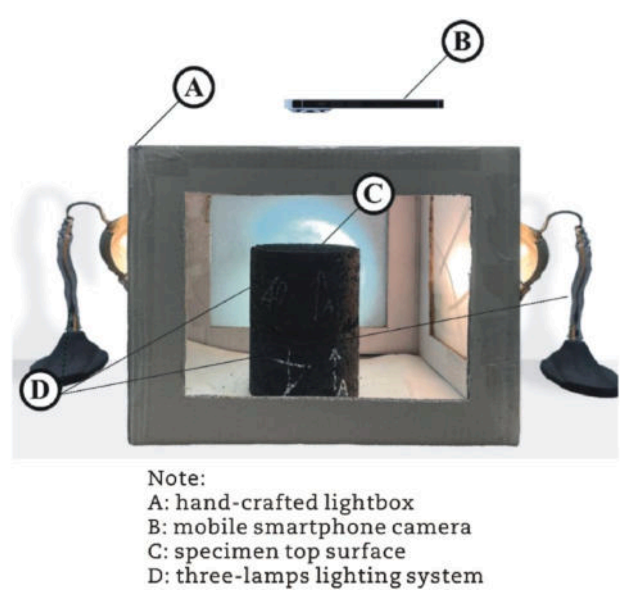

Fig. 2 – Photographic equipment setup.

was located with the camera pointing downwards and fixed to the lightbox top plane. Each specimen was consequently placed at the centre of the box with its top surface approximately 20 ± 1 cm far from the camera, and rotated 15° consecutively in the same direction for every photo, completing a full rotation in approximately 25 shots. This process ensured that each image was captured with at least 60% forward and 30% side overlap with the adjacent images of the surface. The specimen was then lifted by means of a spacer in order to obtain a distance of 10 ± 1 cm from the mobile phone camera, following the same shooting procedure. In this way, the total number of photos composing a set was in the range of 45 ± 5 photos. The first set was necessary to provide a proper digital description of the specimen's shape into the algorithm; the second one was required to introduce a higher level of detail in the images. Lens aperture was set to f/10 in each shot, to provide an adequate depth of field without introducing noise points in the images. To exclude micromotion blur effects due the finger pressure on the screen, a 3 s timer was used. In the end, the focus was set manually on the top peaks of aggregates in every shot. To allow the scaling operations, a series of six control dots was marked on the top surface of the specimens by means of a framework, creating a pseudo-triangular shape with the side of 5 ± 0.01 cm in the central portion of the specimen. The procedure was repeated in the same way on each specimen, collecting a database that included over 2500 pictures.

Each set of images was post-elaborated using the proprietary software 3DF Zephyr Pro v. 6.509 (3DFlow, Verona, Italy), which is a Structure from Motion photogrammetry pipeline software that includes in-built algorithms for the extraction of 3D models from pictures and videos, also allowing measurements and post processing of data. The importing phase included lens and camera calibration using specific datasets provided by phone manufacturer, to compensate the perspective distortion and the vignetting effect, and the masking of the photos. The latter operation was performed manually by using the 3DF Masquerade tool to exclude from the algorithm computation the external points belonging to the background. A sparse cloud of points was preliminary created to define the reference relative positioning system among the pictures composing a set. Software was set to use an incremental pipeline reconstruction algorithm, selected between those internally provided, using the highest available sensitivity for keypoints generation and matching. A dense cloud of points was then generated referring to the sparse cloud, using software in-built epipolar line and hyperplane algorithms for point generation and matching. An average of 1,200,000 ± 100,000 points cloud was obtained for each specimen, resulting in a resolution of approximately 7000 points/cm^2. To interpolate the dense cloud, in order to obtain a continuous surface, a textured mesh was created, offering a realistic and faithful reconstruction of specimen's top surface, as shown in Fig. 3. Besides providing photoconsistency in the model, textured mesh extraction was required to ease levelling and scaling phases minimizing computational errors. The 3D model was horizontally re-oriented and scaled referring to the six-control points system marked on the specimens and converted into a xyz matrix of coordinates. More specifically, the distance between two consecutive sides was used as constraint length, and the third one as control distance. The average computational error was measured in 0.02 ± 0.01 mm, comparing real scaling system dimensions and the digital output measures.

The 3D models were then imported as xyz matrix in the proprietary software MountainsMap Premium v 9.3.10281 (Digital Surf, Besançon, France), for the surface texture analysis. To avoid any edge effect, possibly caused by external edge irregularities, a circular area having a diameter of 100 mm was selected for the analysis in the central portion of the specimens. Before proceeding with texture calculation, the extracted area was horizontally levelled using the least-mean square plane (LSPL) algorithm. Furthermore, the general form was suppressed to exclude any rippling surface (Woodward et al., 2014), by applying a square-polynomial form suppression inner algorithm, provided by the software. Finally, a thresholding operator was applied to remove minor spikes caused by light reflection on the crystalline portion of aggregates (Kogbara et al., 2018), cutting a small depth from the highest peak (average material ratio excluded approximately of 0.03%), based on height distribution histogram's effective starting point. The above-described procedure is represented in Fig. 4.

Fourteen texture parameters were considered for the surface characterization, concerning ISO 25178-23 classification, including height, volume and distribution of statistical and

Fig. 3 – Close-range photogrammetry 3D-model generation.

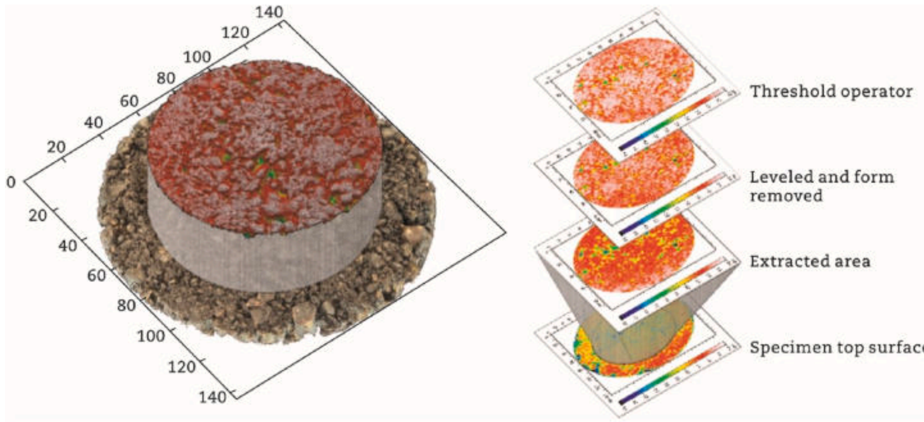

Fig. 4 – Surface texture generation (unit: mm).

intrinsic indicators. Texture parameters were selected from a longer list and automatically calculated using the in-built algorithms included in the MountainsMap software. A brief description and a graphical representation of all parameters is provided in Table 2 (Callai and Sangiorgi, 2021; Olympus-IMS, 2023).

2.4. *Volumetric patch test*

For the reasons previously introduced, volumetric patch test was selected for the empirical assessment of surface macro-texture. The conventional volumetric approach expresses macro-texture as the mean texture depth (MTD) value, defined as the ratio between a constant volume of material, monogranular sand or glass spheres, and the variable area covered by spreading it over the pavement surface. The application of this methodology on laboratory manufactured specimens required its adaptation, however it is based on the same principle and the equipment included in EN 13036-1. The specimen was placed inside a pan on a laboratory scale, sensitive to 0.01 g. A standard cylindrical container, having a nominal "unit volume" V_U of 25,000 ± 150 mm^3, was filled with graded monogranular sand recording the weight of the material inside it as the "weight of the unit volume" W_U. The sand was then poured at the centre of the specimen's top surface and carefully spread using the rubber spreading tool until the whole surface was covered, having care that every excess of sand fell inside the pan. Removing the sand-covered specimen, Fig. 5, it was possible to record the "weight of the excess sand" W_{ES} directly reading the value on the scale. The "volume of the excess sand" V_{ES} was then calculated by using the relation.

$$V_{ES} = \frac{W_{ES} V_U}{W_U} \tag{1}$$

where V_{ES} is the volume of the excess sand (mm^3), W_{ES} is the weight of the excess sand (g), V_U is the unit volume of sand (mm^3), W_U is the weight of a unit volume (g).

In case of highly-textured specimens, for those where the V_U was insufficient to cover the whole surface, the unit volume was doubled or tripled. The "volume of the retained sand" V_{RS} was then calculated as follow.

$$V_{RS} = N_{V_U} V_U - V_{ES} \tag{2}$$

where V_{RS} is the volume of the retained sand (mm^3), V_{ES} is the volume of the excess sand (mm^3), V_U is the unit volume of sand (mm^3), N_{V_U} is the number of unit volume of sand used.

Finally, the mean texture depth (MTD) was expressed as follow.

$$MTD = \frac{V_{RS}}{A} \tag{3}$$

where MTD is the mean texture depth (mm), A is the area of the specimen (mm^2).

2.5. *Pendulum test*

To estimate the micro-texture properties of the specimens, the pendulum test was selected and performed in accordance with EN 13036-4. An appropriate locking system, consisting in clamps and stable supports, was used to avoid any movement of the specimen during the test. The test was performed in wet conditions, ensuring a contact area equal to the standard sliding length of 126 ± 1 mm and avoiding any contact with the edge of the specimen. To minimize the empirical correction prescribed in Table 3 of EN 13036-4, specimens, rubber slider and water were conditioned in a climate chamber at 20 °C for at least 4 h before performing the test. "Pendulum test value" (PTV), which expresses the energy loss during the sliding, was calculated as the mean of five consecutive swings using the formula as follow.

$$PTV = \frac{\sum_{i=1}^{5} \nu_i}{5}$$

where ν_i is the individual values for each swing.

3. Analysis of results

In order to extend the field of applicability of the proposed methodology, ensuring the texture variability of the tested pavement was essential. In this regard, the results of volumetric patch test and pendulum test, shown in Fig. 6(a) and (b)

Table 2 – Texture parameters description.

Parameter		Formula	Graphical explanation
Sa	Mean surface roughness	$\frac{1}{A}\iint\lvert Z(x,y\rvert dxdy$	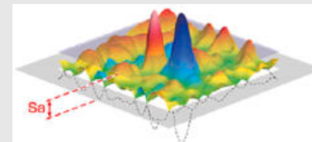
It represents the average deviation of the surface over a defined area (Medeiros et al., 2021). It expresses the average elevation between positive and negative points form the mean plane.			
Sq	Root mean square height	$\sqrt{\frac{1}{A}\iint Z^2(x,y)dxdy}$	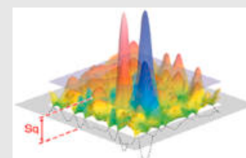
This parameter represents the root-mean square value of ordinate values in the area (Kogbara et al., 2018).			
Sz	Maximum surface height	Sp + Sv	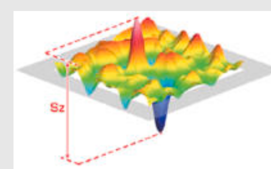
It is the maximum peak to valley height measured over the area, expressing the distance between the highest peak and the lowest valley (Michigan Metrology-LLC-Livonia (MI), 2014), where Sp and Sv are the maximum peak height and the maximum valley depth, respectively.			
Vmp	Peak material volume	–	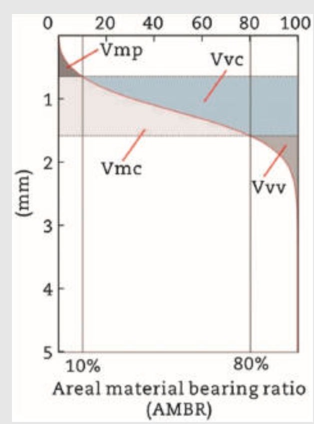
Like the other volumetric parameters, it can be obtained from the bearing area curve (BAC), often known as Abbott-Firestone curve (Ech et al., 2009). It represents the volume of material corresponding to a 10% material-bearing ratio level to the highest peak (Medeiros et al., 2021). It can be associated to the volume of material that may be worn away and characterize the contact zone (Kogbara et al., 2018).			
Vmc	Core void volume	–	
It is the volume of material comprising heights between 10% and 80% of the material-bearing ratio. It represents the volume of material available after the peaks of the surface is worn (Kogbara et al., 2018).			
Vvc	Valley void volume	–	
It represents the space bounded by texture at heights corresponding to the material ratio of 10% and 80%, respectively (Michigan Metrology-LLC-Livonia (MI), 2014).			
Vvv	Core material volume	–	
It is the volume of space bounded by the surface texture from a chosen plane and the lowest valley (Michigan Metrology-LLC-Livonia (MI), 2014).			
Sku	Kurtosis	$\frac{1}{Sq^4}\left[\frac{1}{A}\iint Z^4(x,y)dxdy\right]$	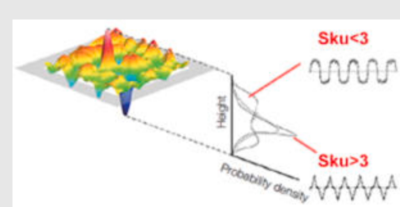

(continued on next page)

Table 2 – (*continued*)

Parameter		Formula	Graphical explanation
It is a function representing the height of the surface relative to the best fitting plane (Hu et al., 2016). When kurtosis is equal to 3, the distribution will have the same shape of a Gaussian distribution. Where Sku is higher than 3 the curve is really sharp, whereas if it much lower the curve becomes rounded and flatted (Callai et al., 2022).			
Ssk	Skewness	$\frac{1}{Sq^3}\left[\frac{1}{A}\iint Z^3(x,y)dxdy\right]$	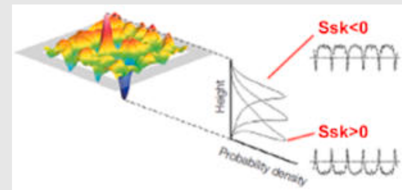
It is a function representing the height of the surface relative to the best fitting plane (Hu et al., 2016). Skewness assumes a value equal to 0 if the probability density curve of the profile is symmetrical. Higher or lower number of peaks above the average will make the Ssk negative or positive, respectively (Callai et al., 2022).			
Sk	Depth of working surface	–	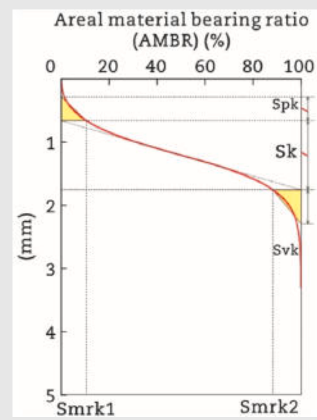
It is the difference of heights at the material ratio of 0% and 100% on the equivalent line, and it can be obtained by subtracting the minimum height from the maximum height of the core surface.			
Spk	Amplitude of peaks	–	
It represents the mean height of peaks above the core surface.			
Svk	Depth of valleys	–	
It is an indicator of the magnitude of valleys and expresses the arithmetical mean of the reduced valley depth of an aerial material ratio curve.			
Smk1	Peak material portion	–	
It is defined as the fraction of surface that consists in small peaks above the profile plateau (Ech et al., 2009).			
Smk2	Core material portion	–	
It is defined as the fraction of surface that can support a load during the service life (Ech et al., 2009).			

respectively, are sorted in ascending order to emphasize the micro- and macro-texture differences among the investigated surfaces.

As previously discussed in the introduction section, MTD and PTV are extrinsic parameters based on aggregate criteria (Praticò et al., 2003), which both refer to the overall effect produced by the totality of the surveyed wavelengths on texture. For this reason, their values were expected to present a different sensibility to morphological changes within different wavelength ranges of definition. In the light of above, the results of empirical tests were compared with those of CRP analysis by means of an individual pairwise comparison between the parameters.

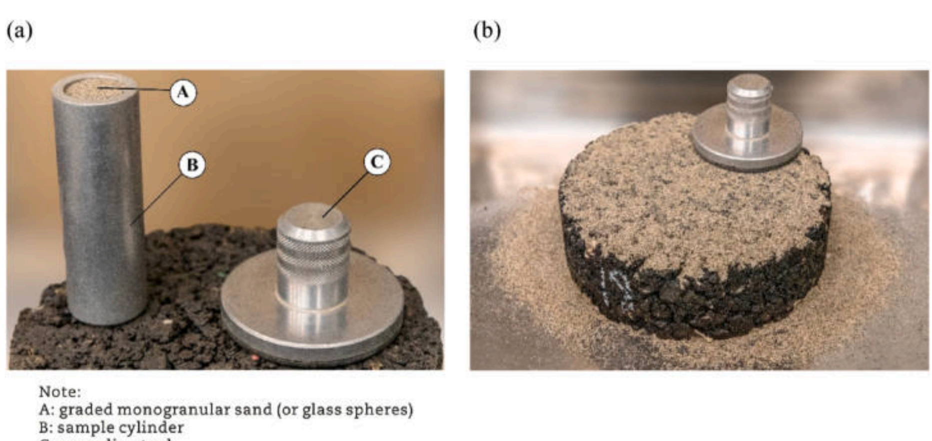

Fig. 5 – Volumetric patch test. (a) Equipment. (b) Test execution.

Table 3 – Correlation coefficient R^2 between texture parameters.

R^2	MTD	PTV	Vmp	Vmc	Vvc	Vvv	Sa	Sq	Sz	Ssk	Sku	Sk	Spk	Svk	Smrk1	Smrk2
MTD	1	0.0663	0.3925	0.9572	0.9500	0.9210	0.9533	0.9458	0.7682	0.1172	0.1179	0.9183	0.0461	0.9309	0.2573	0.3424
PTV		1	0.0549	0.0732	0.0746	0.0480	0.0665	0.0584	0.0424	0.0503	0.0078	0.0729	0.0230	0.0521	0.0024	0.0039
Vmp			1	0.4304	0.5065	0.4634	0.4543	0.4740	0.4296	0.0519	0.0258	0.5297	0.7805	0.4665	0.0092	0.0131
Vmc				1	0.9903	0.9735	0.9977	0.9898	0.8175	0.1515	0.1556	0.9670	0.0565	0.9757	0.3080	0.4043
Vvc					1	0.9705	0.9925	0.9880	0.8041	0.1555	0.1513	0.9892	0.0939	0.9718	0.2553	0.3323
Vvv						1	0.9859	0.9939	0.8366	0.0900	0.1117	0.9496	0.0754	0.9982	0.2713	0.4007
Sa							1	0.9969	0.8261	0.1336	0.1418	0.9709	0.0678	0.9873	0.2900	0.3947
Sq								1	0.8401	0.1044	0.1154	0.9655	0.0786	0.9957	0.2660	0.3832
Sz									1	0.0257	0.0336	0.7755	0.0906	0.8421	0.2198	0.3866
Ssk										1	0.9087	0.1857	0.0025	0.0803	0.2248	0.0831
Sku											1	0.1800	0.0014	0.0974	0.3531	0.1933
Sk												1	0.1067	0.9452	0.2645	0.2964
Spk													1	0.0774	0.2164	0.0410
Svk														1	0.2523	0.3892
Smrk1															1	0.6579
Smrk2																1

In volumetric patch test results a near linear correlation with Sa and Sq was found, as shown in Fig. 7(a) and (b), since they both relate to surface mean plane in a macro-texture range, sharing the same principle of MTD. The correlation between MTD and Sz, which is still significant and presents a $R^2 > 0.75$ (Fig. 7(c)), is slightly lower being Sz possibly influenced by local peaks/valleys effects and not being representative of the whole surveyed area.

Moreover, MTD is also highly correlated with the volumetric parameters Vmc, Vvc and Vvv (Fig. 8), which all describe the volume shaped by surface texture between the deepest valley and the post-peak portion, according with other studies (Li et al., 2017). Those values reflect the empty volume available to be filled with sand, so the high correlation was expected and it confirms the reliability of the surface modelling procedure. Vmp, which refers to the volume of the highest peaks, presents a weaker direct relationship with MTD.

The trend is respected by comparing MTD with the Sk-parameters, where a high correlation with Sk and Svk, which are descriptive of surface core and valleys, clearly appears (Fig. 9(b) and (c)). On the contrary, the amplitude of peaks Spk does not seem to influence MTD (Fig. 9(a)). A motivation to this could be that the peaks amplitude, which ranged between 0.07 and 0.37 mm, felt in a micro-texture range. The volumetric patch approach, which makes use of monogranular sand with a diameter of 0.2 mm, may not be sensitive enough to appreciate the micro-peaks appearing on the surface.

In the end, feature parameters Ssk, Sku, Smk1 and Smk2 resulted independent from MTD. This determined that volumetric patch test could quantify but not qualify texture, since was not able to discriminate between surfaces presenting different texture polarity, density and orientation.

No significant differences were observed by varying the colour of the surfaces, excluding the hypothesis of dependency from light reflections and thermal noise, with the testing setup adopted. In addition, all above mentioned correlations did not show trend deviations in any texture range, proving the effectiveness of the lighting system into avoiding shadowing effects on photographs.

The complete correlation matrix, which includes the pairwise comparison between all the above-described texture parameters expressed by means of the correlation coefficient R^2, is shown in Table 3.

It can be also observed that roughness height parameters (Sa, Sq, Sz) show a high correlation between themselves, in accordance with other previous studies (Qian and Meng, 2017; Vaiana et al., 2019).

On the other hand, no significant relationship between the frictional coefficient PTV and the other texture parameters was eventually found. This confirms that Pendulum Test, which is an indirect texture assessment methodology, might be influenced by other factors than geometrical texture (Chu et al., 2019; Pancar and Karaca, 2016). Other studies already found weak correlations between topographical and friction parameters in assessing texture (Cafiso and Taormina, 2007; Shalaby and El Gendy, 2012; Yu et al., 2020) observed a very low dependency of macro-texture on pendulum test and (Torbruegge and Wies, 2015) demonstrated the absence of correlation between MTD and PTV (Mahboob et al., 2015). Established a low direct relationship between Sq, Ssk and

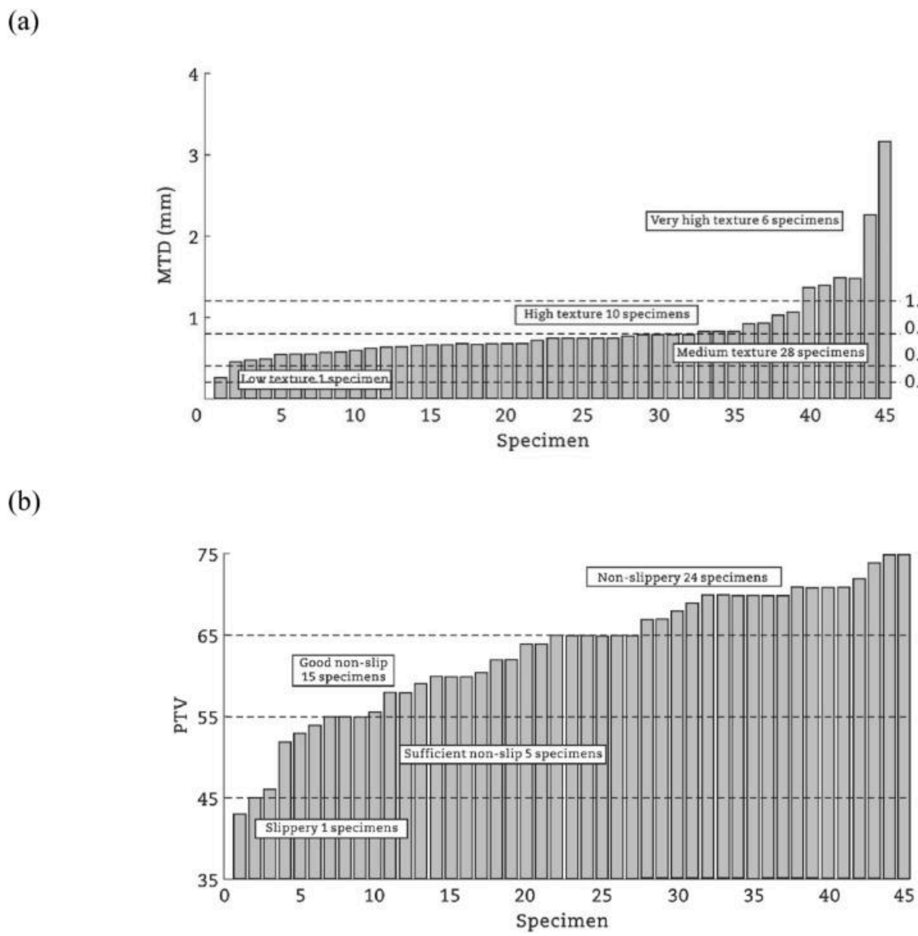

Fig. 6 – Results of empirical tests. (a) Results of volumetric patch test. (b) Results of pendulum test.

friction. (Qian and Meng, 2017) found no correlations between PTV and roughness parameters Sa, Sq, Sz, Sku, Ssk calculated with a 3D laser microscope. In the light of the above, the lacking of relationship between texture parameters and PTV was expected and cannot be ascribed to the analysis methodology, but to Pendulum Test itself.

4. Conclusions

This study proposed a simple and low-budged methodology for the laboratory and in-situ assessment of surface texture with a contactless approach. The main aim was to define a procedure for its implementation as a tool for pavements applications, presenting a workflow to use it with an ordinary mobile phone camera. To evaluate the reliability and the replicability of the method a large number of existing wearing course materials was tested. The comparison with two common empirical approaches for surface texture evaluation was conducted and discussed. Based on the obtained results and the related analyses, the following main conclusions can be drawn.

- Close-range photogrammetry can be successfully adopted for road pavements surface 3D texture analysis. If compared with other non-contact methodologies, it can drastically decrease the costs of the equipment required for maintenance.
- Data acquisition procedure implemented in this study was proven to be adequate to override the quality gap with expensive testing equipment, as witnessed by the high correlated results obtained. The use of an ordinary mobile phone camera resulted in a reliable and valid possibility.
- MTD exhibited a high relationship with height roughness parameters Sa, Sq and Sz ($R^2 = 0.95, 0.94, 0.77$, respectively). It also well correlated with the volume parameters Vmc, Vvc and Vvv ($R^2 = 0.95, 0.95, 0.91$, respectively) and with Abbott-Firestone curve Sk-parameters in the post-peaks to valleys range, representative of macro-texture.
- MTD did not correlate with feature parameters Sku, Ssk, Smk1 and Smk2, demonstrating to be inadequate for a qualitative assessment of macro-texture, while a quantitative reliability was confirmed. Moreover, it was found to be independent from peaks portion of texture, confirming a low effectiveness of Volumetric Patch Test on highly-microtextured surfaces.
- Low-correlations were found comparing PTV with all other intrinsic texture parameters. The sensibility of Pendulum Test to aspects beyond the pure geometrical texture was confirmed.

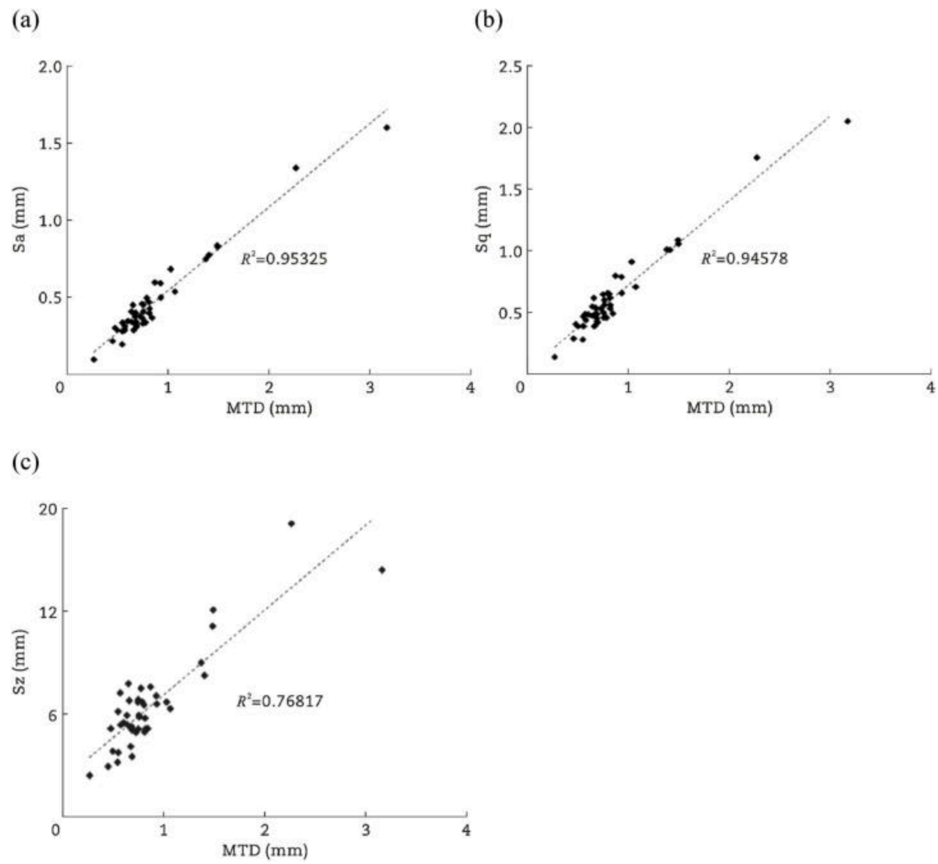

Fig. 7 – Correlation. (a) MTD-Sa. (b) MTD-Sq. (c) MTD-Sz.

5. Discussion and further research

While on one hand, empirical approaches are helpful for a preliminary classification of road pavements, on the other hand, they may lead to poorly detailed texture description and to a limited overall description of the surface. The use of close-range photogrammetry analysis can ease the surface characterization of road pavements in ordinary and complex scenarios, not aiming to replace the conventional approaches, but to integrate them introducing few additional operator skills and low budget equipment. The strong correlations found analysing the 3D models of the surfaces showed the reliability of the method and the depth of detail obtainable with this technique, thus giving the possibility to increase the control on pavements status, especially to monitor their evolution in time for maintenance purposes. The weak correlations with skewness (Ssk) and kurtosis (Sku) also demonstrated how the volumetric patch test cannot be appropriate to appreciate the polarity and the orientation of surface texture, which are crucial factors in acoustic, frictional and optical problems. While volumetric patch test remains a valid and rapid tool for a quantitative evaluation of texture, this study demonstrated its inadequacy in more complex problems, where quality of texture is also a key factor. Moreover, it was shown how the reliability of its results decreases over a certain level of spatial frequency, proving that volumetric patch test should not be considered on pavements where micro-texture domain is dominant. Low dependency of pendulum test results on texture parameters highlighted the limitations of extrinsic methods for the morphological description of pavements. PTV confirmed to be highly-interpretable in certain applications, since does not take into account the individual contributes of macro-texture (hysteresis) and micro-texture (adhesion) to the total friction measurement. This study demonstrated how performing Pendulum Test on surfaces where macro-undulation is dominant over micro-texture (or vice-versa) may produce ambiguity in the results. The flexibility and the upgradability of the CRP-based methods may be the key to develop new tools based on the dis-aggregate digital analysis of surfaces, consenting to filter the profiles over different wavelengths and quantify the contribution to friction of each texture class. In this regard, authors are already developing an algorithm based on the discrete fourier transform (DFT) that will be implemented in the method to include spectral analysis in the texture description, which will be investigated and discussed in further studies. This will extend morphological analysis of pavements to a more detailed level, including

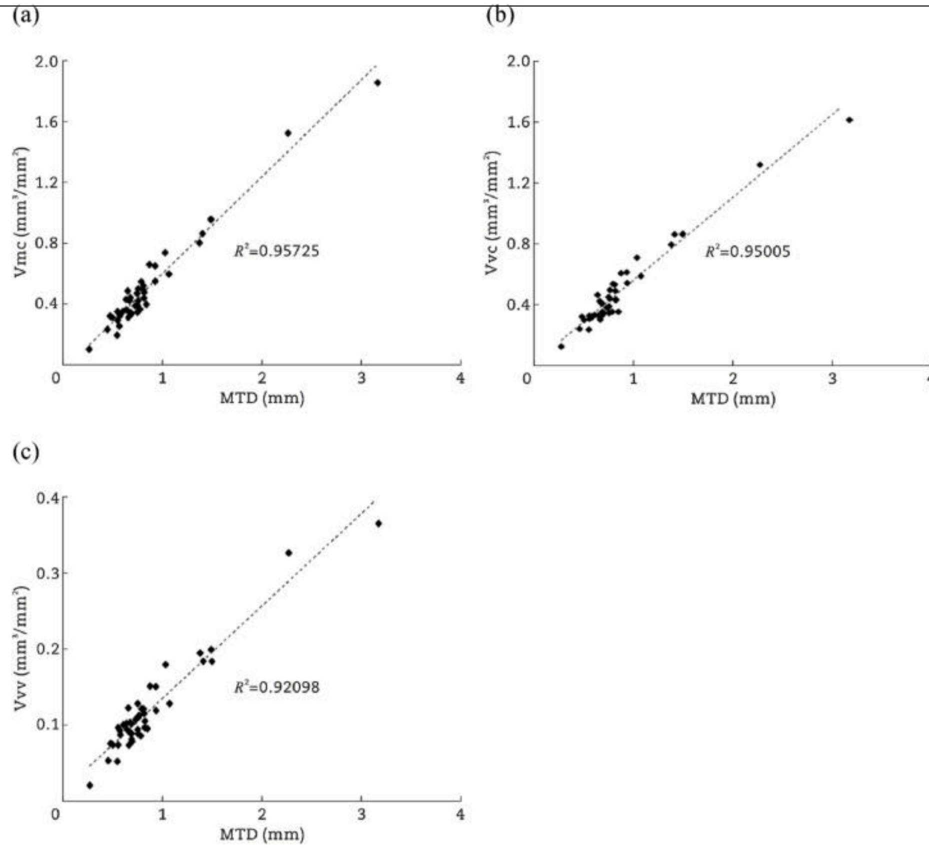

Fig. 8 – Correlation. (a) MTD-Vmc. (b) MTD-Vvc. (c) MTD-Vvv.

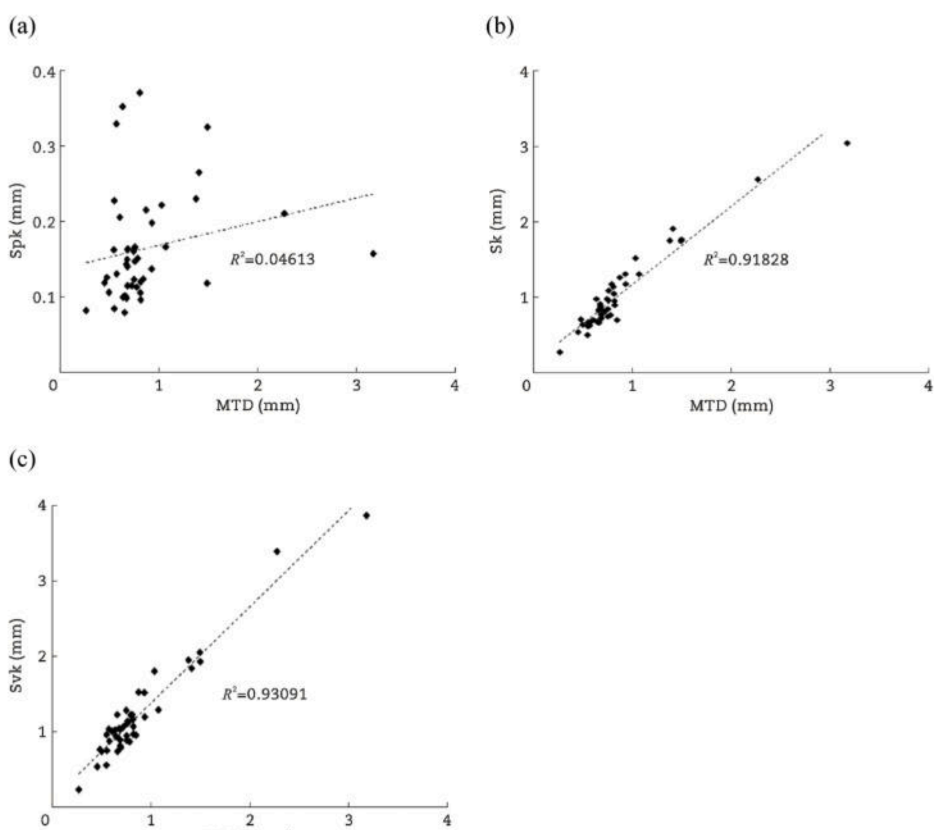

Fig. 9 – Correlation. (a) MTD-Spk. (b) MTD-Sk. (c) MTD-Svk.

new advanced texture related topics, such as water surface runoff or pavement cleaning and painting processes, where the direction, the interconnection and the volume of valleys are key factors. In addition, the authors believe that different approaches need to be verified to evaluate the relationship between conventional and digital texture assessment methodologies, in order to complement the existing standards with clear boundaries of applicability. The use of Micro GripTester will be investigated when the proposed methodology will be implemented for in-situ applications. In this regard, different preliminary transpositions of the method to road pavements have been already successfully tested and will be discussed in future works. In fact, the plainness of the setup allows to directly transpose the above-described technique in-situ, replacing the white background with a simple white paper mask and without the need of the lightning system, in adequate solar illumination conditions. Expanding the dataset of pavements, including those investigated in-situ, is expected to extend the field of application of the proposed methodology and to refine the correlations found.

Conflict of interest

The authors do not have any conflict of interest with other entities or researchers.

CRediT authorship contribution statement

Filippo Balzano: Writing – original draft, Investigation, Formal analysis, Data curation. **Piergiorgio Tataranni:** Writing – review & editing, Supervision. **David Woodward:** Writing – review & editing, Methodology, Conceptualization. **Cesare Sangiorgi:** Writing – review & editing, Supervision, Conceptualization.

Data availability statement

The data that support the findings of this study are available from the corresponding author, upon reasonable request.

Acknowledgments

The authors would like to gratefully acknowledge all the technicians of LAS laboratory of the University of Bologna for their precious contribute during the experimental phase.

REFERENCES

Afonso, M.L., Dinis-Almeida, M., Fael, C.S., 2019. Characterization of the skid resistance and mean texture depth in a permeable asphalt pavement. IOP Conference Series: Materials Science and Engineering 471 (2), 022029.

Ansary, T.F., Daoudi, M., Vandeborre, J.-P., 2007. A Bayesian 3-D search engine using adaptive views clustering. IEEE Transactions on Multimedia 9 (1), 78–88.

Ban, I., Deluka-Tibljaš, A., Cuculić, M., 2022. Orthographic photogrammetry method for pavement texture characterization. Road and Rail Infrastructure 7, 325–331.

Biao, L., Zeng, J., Yao, M., et al., 2015. 3D object retrieval with multitopic model combining relevance feedback and LDA model. IEEE Transactions on Image Processing 24 (1), 94–105.

Bitelli, G., Simone, A., Girardi, F., et al., 2012. Laser scanning on road pavements: a new approach for characterizing surface texture. Sensors (Switzerland) 12 (7), 9110–9128.

Boscaino, G., Giunta, M.S., Vaiana, R., 2002. Tessitura superficiale di manti stradali: Indicatori da acquisizione profilometrica con metodo non-contact. In: XII Convegno Nazionale Stradale AIPCR, St Vincent (AO), 2002.

Canestrari, F., Mariani, E., Ingrassia, L.P., 2024. Use of Wehner-Schulze machine to evaluate pavement skid resistance: a review. Journal of Traffic and Transportation Engineering (English Edition) 11 (5), 896–917.

Cafiso, S., Taormina, S., 2007. Texture analysis of aggregates for wearing courses in asphalt pavements. International Journal of Pavement Engineering 8 (1), 45–54.

Callai, S.C., De Rose, M., Tataranni, P., et al., 2022. Microsurfacing pavement solutions with alternative aggregates and binders: a full surface texture characterization. Coatings 12 (12), 2121905.

Callai, S.C., Sangiorgi, C., 2021. A review on acoustic and skid resistance solutions for road pavements. Infrastructures 6 (41), 6030041.

CEN, 2010. Road and Airfield Surface Characteristics-Test Methods. Part 1: Measurement of Pavement Surface Macrotexture Depth Using a Volumetric Patch Technique. EN 13036-1. European Committee for Standardization, Brussel.

CEN, 2011. Road and Airfield Surface Characteristics-Test Methods Part 4: Method for Measurement of Slip/skid Resistance of a Surface: the Pendulum Test. EN 13036-4. European Committee for Standardization, Brussel.

Cesbron, J., Anfosso-Lédée, Yin, P., et al., 2008. Influence of road texture on tyre/road contact in static conditions. Road Materials and Pavement Design 9 (4), 689–710.

Chen, J., Huang, X., Zheng, B., et al., 2019. Real-time identification system of asphalt pavement texture based on the close-range photogrammetry. Construction and Building Materials 226, 910–919.

Chu, L., Cui, X., Zhang, K., et al., 2019. Directional Skid Resistance Characteristics of Road Pavement: Implications for Friction Measurements by British Pendulum Tester and Dynamic Friction Tester. Transportation Research Board, Washington DC.

Cooley, L.A., 1999. Permeability of Superpave Mixtures-Evaluation of Field Permeameters. National Center for Asphalt Technology, Auburn.

Dong, S., Han, S., Wu, C., et al., 2022. Asphalt pavement macrotexture reconstruction from monocular image based on deep convolutional neural network. Computer-Aided Civil and Infrastructure Engineering 37 (13), 1754–1768.

Ech, M., Morel, S., Yotte, S., et al., 2009. An original evaluation of the wearing course macrotexture evolution using the Abbot curve. Road Materials and Pavement Design 10 (3), 471–494.

Fernando, E.G., Hu, S., Crockford, W., 2023. Comparative evaluation of pavement macrotexture measurements from different devices. Transportation Research Record 2677, 782–796.

Gao, Y., Dai, Q., 2014. View-based 3D object retrieval: challenges and approaches. IEEE MultiMedia 21 (3), 52–57.

Gu, F., Chen, C., Heitzman, M., et al., 2022. Evaluation of locked-wheel skid trailer and SCRIM friction measurements at

NCAT test track. International Journal of Pavement Engineering, https://doi.org/10.1080/10298436.2022.2124249.

Hao, X., Sha, A., Sun, Z., et al., 2016. Evaluation and comparison of real-time laser and electric sand-patch pavement texture-depth measurement methods. Journal of Transportation Engineering 142 (7), 0000842.

Hoang, N.D., 2019. Automatic detection of asphalt pavement raveling using image texture based feature extraction and stochastic gradient descent logistic regression. Automation in Construction 105, 102843.

Hu, L., Yun, D., Liu, Z., et al., 2016. Effect of three-dimensional macrotexture characteristics on dynamic frictional coefficient of asphalt pavement surface. Construction and Building Materials 126, 720–729.

Ioannidou, A., Chatzilari, E., Nikolopoulos, S., et al., 2017. Deep learning advances in computer vision with 3D data: a survey. ACM Computing Surveys 50, 3042064.

Kogbara, R.B., Masad, E.A., Kassem, E., et al., 2016. A state-of-the-art review of parameters influencing measurement and modeling of skid resistance of asphalt pavements. Construction and Building Materials 114, 602–617.

Kogbara, R.B., Masad, E.A., Woodward, D., et al., 2018. Relating surface texture parameters from close range photogrammetry to Grip-tester pavement friction measurements. Construction and Building Materials 166, 227–240.

Leng, B., Liu, Y., Yu, K., et al., 2016. 3D object understanding with 3D convolutional neural networks. Information Sciences 366, 188–201.

Leng, Z., Fan, Z., Liu, P., et al., 2023. Texturing and evaluation of concrete pavement surface: a state-of-the-art review. Journal of Road Engineering 3 (3), 252–265.

Li, W., Bebis, G., Bourbakis, N.G., 2008. 3-D object recognition using 2-D Views. IEEE Transactions on Image Processing 17 (11), 2236–2255.

Li, Q., Song, S., Wang, J., et al., 2024. A review of the development of asphalt foaming technology. Journal of Road Engineering 4 (3), 334–347.

Li, Q., Yang, G., Wang, C., 2017. Three-dimensional-based areal texture parameters for pavement friction. In: Transportation Research Board 96th Annual Meeting, Washington DC, 2017.

Liu, C., Li, J., Gao, J., et al., 2021. Three-dimensional texture measurement using deep learning and multi-view pavement images. Journal of the International Measurement Confederation 172, 108828.

Luhmann, T., Fraser, C., Maas, H.G., 2016. Sensor modelling and camera calibration for close-range photogrammetry. ISPRS Journal of Photogrammetry and Remote Sensing 115, 37–46.

Luo, H., Chen, S., Zhu, L., et al., 2023. Investigation of surface textures deterioration on pavement skid-resistance using hysteresis friction models and numerical simulation method. Friction 2023 (41), 1–35.

Mahboob Kanafi, M., Kuosmanen, A., Pellinen, T.K., et al., 2015. Macro-and micro-texture evolution of road pavements and correlation with friction. International Journal of Pavement Engineering 16 (2), 168–179.

Mathavan, S., Kamal, K., Rahman, M., 2015. A review of three-dimensional imaging technologies for pavement distress detection and measurements. IEEE Transactions on Intelligent Transportation Systems 16 (5), 2353–2362.

Medeiros, M., Babadopulos, L., Maia, R., et al., 2021. 3D pavement macrotexture parameters from close range photogrammetry. International Journal of Pavement Engineering 24 (2), 2020784.

Michigan Metrology-LLC-Livonia (MI), 2014. Surface Texture Parameters Glossary. Available at: https://michmet.com/surface-texture-parameters-glossary/ (Accessed 12 July 2023).

Miljković, M., Radenberg, M., Gottaut, C., 2014. Characterization of noise-reducing capacity of pavement by means of surface texture parameters. Journal of Materials in Civil Engineering 26 (2), 240–249.

National Academies of Science Engineering and Medicine, 2009. Guide for Pavement Friction. The National Academies Press, Washington DC.

Noyce, D.A., Hussain Bahia, P.U., Yambó Guisk Kim, J.M., 2005. Incorporating Road Safety into Pavement Management: Maximizing Asphalt Pavement Surface Friction for Road Safety Improvements. Midwest Regional University Transportation Center, Madison.

Olympus-IMS, 2023. Industrial Microscopes Surface Roughness Measurement-parameters. Available at: https://www.olympus-ims.com/en/metrology/surface-roughness-measurement-portal/parameters (Accessed 15 August 2023).

Pancar, E.B., Karaca, Z., 2016. Reliability of British pendulum test on macrotextured surfaces. International Journal of Innovation Sciences and Research 5 (1), 611–616.

Pranjić, I., Deluka-Tibljaš, A., 2022. Pavement texture–friction relationship establishment via image analysis methods. Materials 15 (3), 15030846.

Praticò, F.G., Vaiana, R., 2015. A study on the relationship between mean texture depth and mean profile depth of asphalt pavements. Construction and Building Materials 101, 72–79.

Praticò, F., Vaiana, R., Boscaino, G., 2003. Spectral texture indicators significance in relation to flexible pavements surface performance. In: XXII World Road Congress-PIARC, Durban, 2003.

Qian, Z., Meng, L., 2017. Study on micro-texture and skid resistance of aggregate during polishing. Frontiers of Structural and Civil Engineering 11 (3), 346–352.

Queiroz, C., Haas, R., Cai, Y., 1994. National economic development and prosperity related to paved road infrastructure. Transportation Research Record 1455, 147–152.

Ramírez-Hernández, L.R., Rodríguez-Quiñonez, J.C., Castro-Toscano, M.J., et al., 2020. Improve three-dimensional point localization accuracy in stereo vision systems using a novel camera calibration method. International Journal of Advanced Robotic Systems 17 (1), 1729881419896717.

Shalaby, A., El Gendy, A., 2012. 3D Pavement surface macrotexture: measurements and friction relationships. In: 7th Symposium on Pavement Surface Characteristics (SURF), Norfolk, 2012.

Torbruegge, S., Wies, B., 2015. Characterization of pavement texture by means of height difference correlation and relation to wet skid resistance. Journal of Traffic and Transportation Engineering (English Edition) 2 (2), 59–67.

Vaiana, R., Balzano, F., Iuele, T., et al., 2019. Microtexture performance of EAF slags used as aggregate in asphalt mixes: a comparative study with surface properties of natural stones. Applied Sciences (Switzerland) 9 (15), 9153197.

Woodward, D., Friel, S., 2017. Predicting the wear of high friction surfacing aggregate. Coatings 7 (5), 7050071.

Woodward, D., Mcquaid, G., Millar, P., 2014. A comparison of techniques to determine surface texture data. In: Civil Engineering Research in Ireland, Belfast, 2014.

Yu, D., Cao, Y., Zhao, Q., 2023. Detection and analysis of asphalt pavement texture depth based on digital image analytics technology. International Journal of Pavement Research and Technology 18, 628–631.

Yu, M., You, Z., Wu, G., et al., 2020. Measurement and modeling of skid resistance of asphalt pavement: a review. Construction and Building Materials 260, 119878.

Yun, D., Hu, L., Sandberg, U., et al., 2025. Skid resistance performance and texture lateral distribution within the lanes of asphalt pavements. Journal of Traffic and Transportation Engineering (English Edition) 12 (1), 87–107.

Filippo Balzano is currently a PhD student at the University of Bologna (Italy), where he is serving as a researcher at the Department of Civil, Chemical, Environmental and Materials Engineering. He obtained both of his bachelor's and master's degrees in civil engineering at the Università della Calabria (Italy), where he specialized in road pavement construction and maintenance. His field of expertise lies in the development of new technologies for the assessment and for validation of innovative compounds, which aim to reduce the need of energy and virgin materials in the transport engineering activities. The use of recycled materials and low impact solutions are also of primary importance in his research. He is the author or co-author of papers for international academic journals and currently member of RILEM and SIIV associations.

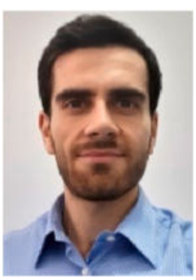

Piergiorgio Tataranni is a post-doc research fellow (junior assistant professor-fixed-term) at DICAM of the University of Bologna. Since 2013 his activity in the roads section of the department has been focused on themes related to pavement materials and construction technologies for civil infrastructures. His research is mainly centred on the development of innovative and sustainable materials and low impact construction technologies. On these topics, he is the author of several scientific publications, his PhD thesis and he participated in Europeans projects as Early Stage Researcher (H2020, REMINE, MSCA-RISE-2014) and Scientific Manager (SAFERUP! H2020 MSCA ITN-2017).

Dr. David Woodward has 42 years' experience with aggregate and asphalt materials. He is reader in infrastructure engineering at Ulster University and chief scientific officer for R3 Ltd who specialise in Roads, Runways and Racing Circuits around the world. He teaches highway engineering and geology and has been involved in the supervision of over 30 PhD's in aggregates, mixes, waste streams, in-service performance, and new product development. He has over 200 publications and has travelled extensively around the world. He is a member of BSI Committee B/510/5-Road Surface Characteristics, B/505/4–Manhole Tops and a member of the committee that prepared BS 8870-High Friction Surfacing. Research interests include what happens at the tyre/road interface, evolution of surface characteristics, new ways of measuring things using AI and how our roads are now responding to change.

Cesare Sangiorgi is a full professor at the University of Bologna, specializing in pavement engineering materials and sustainable construction technologies, prioritizing recycled materials and low-impact solutions. He fosters student engagement through collaborations with esteemed research institutes. Since 2001, he partnered with the Nottingham Transportation Engineering Centre and expanded collaborations globally. Prof. Sangiorgi led SAFERUP!, recruiting 15 Early Stage Researchers in a consortium of 30 for sustainable urban pavement projects. Presently, he coordinates GreeNexUS, a HORIZON EUROPE project promoting urban greening and infrastructure safety. With numerous research agreements nationally and internationally, he actively contributes to professional associations like SIIV, APSE, iSMARTi, and RILEM, and serves on journal boards and conference committees, publishing extensively in pavement engineering.